Neural Computing and Applications (2022) 34:18143–18154
https://doi.org/10.1007/s00521-022-07463-3

ORIGINAL ARTICLE

Adaptive neural network control of an uncertain 2-DOF helicopter system with input backlash and output constraints

Zhijia Zhao[1] · Weitian He[1] · Jingfeng Yang[2,3] · ZhiFu Li[1]

Received: 27 January 2022 / Accepted: 22 May 2022 / Published online: 13 June 2022

Abstract
This study considers an adaptive neural control for a two degrees of freedom helicopter nonlinear system preceded by system uncertainties, input backlash, and output constraints. First, a neural network is adopted to handle the hybrid effects of input backlash nonlinearities and system uncertainties. Subsequently, a barrier Lyapunov function is introduced to limit the output signals for further ensuring the safe operation of the system. The bounded stability of the closed-loop system is analyzed employing the direct Lyapunov approach. In the end, the simulation and experiment results are provided to demonstrate the validity and efficacy of the derived control.

Keywords 2-DOF helicopter system · Neural network control · Input backlash · Output constraint

1 Introduction

Recently, unmanned aerial vehicles (UAVs) have been widely applied in civil and military areas, owing to the advantages of vertical take-off, hovering, flexibility, and rapid response [1, 2]. However, the helicopter is a highly nonlinear multiple-input multiple-output (MIMO) system with multiple coupling and many internal system parameters are difficult to measure accurately in practical applications [3]. Thus, a stabilized control strategy is urgently developed to ensure the stable robustness of nonlinear helicopter systems.

✉ Zhijia Zhao
zhaozj@gzhu.edu.cn

Weitian He
2112007143@e.gzhu.edu.cn

Jingfeng Yang
yangjf@gz.sia.cn

ZhiFu Li
aulzf@gzhu.edu.cn

[1] School of Mechanical and Electrical Engineering, Guangzhou University, Guangzhou 510006, China

[2] Guangzhou Institute of Industrial Intelligence, Guangzhou 511458, China

[3] Chinese Academy of Sciences, Shenyang 110016, China

In recent decades, various control methodologies have been put forward for controller design of helicopter systems, such as model-based control, linear quadratic regulator (LQR) control, and Q-learning control [4–8]. In [4], a model-based tracking controller was introduced to track reference trajectories for small-scale unmanned helicopters. In [5], a linear quadratic controller was designed by an enhanced performance adaptive technique, and the system's performance and robustness were discussed. In [6], a direct adaptive LQR control with the advantage of the wide operating horizon was introduced to increase the system's stability and robustness. In [7], to handle the LQR problem, a new Q-learning algorithm was constructed utilizing an iteration policy. However, the above-mentioned studies linearized the nonlinear helicopter systems by ignoring the nonlinear portion and couple effects for ease of control design, and the instability and poor performance of the nonlinear helicopter systems in practical applications may arise. Thus, incorporating the nonlinearities into the controller design is necessary.

In such case, various nonlinear control methods, such as robust control, optimal control, adaptive neural network (NN) control and so on, have been developed to tackle the uncertainties in UAV systems [9–13]. In [9], a trigonometric-saturation-function-based position controller was designed to address internal and external disturbances. In [10], an adaptive control was proposed to handle the

trajectory tracking issue of flapping-wing micro aerial vehicles. In [11], an adaptive NN control was introduced to approximate unknown helicopter systems with output constraints and input dead-zone. However, the control design in the above literatures resolved the issue of system uncertainties and nonlinearities, and the effect of input backlash nonlinearity was not considered. Moreover, the effectiveness of the above approach was only validated in simulations without an experimental verification. Recently, some nonlinear control methods have been developed in the practical application of helicopter systems. In [14], an explicit model predictive control was introduced for a helicopter system to track desired time-varying trajectories. In practice, the optimization problems is difficult to be solved in the case of short sampling time intervals. It can be noted that the optimization computation in the predictive control scheme was achieved offline and the effects of internal mechanical properties and external disturbances were neglected. In [15], a sliding mode control (SMC) synthesis was proposed to compensate the effect of the external disturbances and chattering phenomenon often occured under the SMC, which may result in system instabilities or even destruction under long-time operation. Hence, a control scheme with online adjustment and steady operation is necessary for practical application.

Input nonlinearities universally exist in practical engineering applications due to non-smooth mechanical connections [16–22]. Backlash is one of the input nonlinearities, the existence of which may affect the smoothness of input signal and then cause control performance degradation. Thus, it is imperative to develop effective control schemes to handle and compensate for the effects of backlash nonlinearity. In [20], an H-infinity observer-based feedback control was constructed for time-delayed MIMO nonlinear systems to compensate for unknown backlash and estimate unmeasurable states. In [21], a neural network-adaptive strategy was established to address the tracking control for uncertain MIMO nonlinear systems. In [22], a robust H-infinity control was proposed for UAV systems to handle parametric uncertainties including nonlinear friction force and backlash. Although the successful solution has been attained on the control design for tackling the backlash in MIMO systems, little research has been reported thus far on the adaptive NN control for unknown 2-DOF helicopter systems with input backlash, which inspires us for further study.

In practical control engineering, due to the requirement for the stability and security of the system, the signals of states and outputs should be maintained in a reasonably constrained range [23–25]. If the constraints are transgressed and violated, it may give rise to system performance degradation, result in instability, or even lead to serious accidents [26]. Thus, constraints are required to be incorporated into the control design. Barrier Lyapunov function (BLF), as an effective tool to address the constraint issue, was proposed to handle output constraints in nonlinear systems [27]. In [28], the BLF was introduced in the design of adaptive NN control to prevent from violating the constraint. In [29], a novel integral BLF was proposed to address the full state constraints. In [30], time-varying constraints were considered in an adaptive NN control design of n-link robot systems. However, the above study only resolved the output constrained control for nonlinear systems, and the simultaneous effects of the backlash nonlinearity, output constraints, and uncertainties were neglected. Considering the complexly coupled characteristics in 2-DOF helicopter systems will pose an increased challenge to the control design.

Driven by the existing results, this study concentrates on the design of an adaptive NN control of uncertain 2-DOF helicopter systems involving the input backlash and output constraint. The main contributions are summarized as follows:

1. The input backlash, output constraints, and uncertainties are considered in 2-DOF helicopter systems, and the RBFNN is utilized to develop an adaptive NN constrained control to approximate the unknown function and uncertainties, and ensure no violation of constraints.
2. The proposed adaptive NN control can stabilize the closed-loop system at a specified region. The simulation and experiment results on the Quanser's 2-DOF helicopter platform prove the control performance.

2 Problem formulation

A backlash nonlinearity shown in Fig. 1 is depicted as [31]

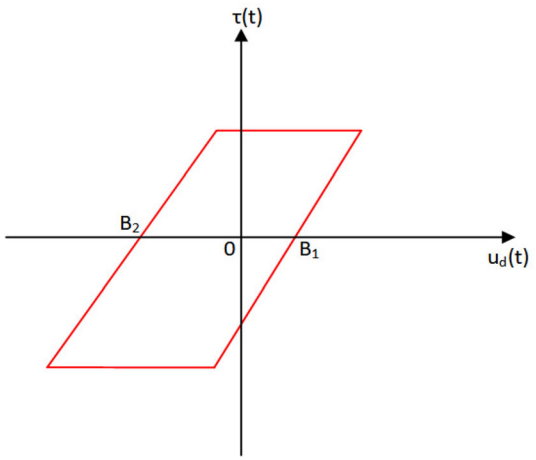

Fig. 1 Backlash diagram

$$\tau(t) = B(u_d) = \begin{cases} \kappa(u_d(t) - B_1), & \text{if} \quad \dot{u}_d > 0 \quad \text{and} \\ & \tau(t) = \kappa(u_d(t) - B_1), \\ \kappa(u_d(t) - B_2), & \text{if} \quad \dot{u}_d < 0 \quad \text{and} \\ & \tau(t) = \kappa(u_d(t) - B_2), \\ \tau(t\_), & \text{otherwise}, \end{cases} \tag{1}$$

where $B(u_d)$ denotes a backlash nonlinearity, $u_d(t)$ is a desired control input, and $\tau(t\_)$ means that the output signal $\tau(t)$ remains unchanged. $\kappa > 0$, $B_1 > 0$, and $B_2 < 0$ are constant parameters. In addition, κ is the line's slope.

Assumption 1 The parameters κ, B_1, and B_2 are known and bounded constants in (1) and satisfy the following constraints

$$\begin{aligned} &0 < \kappa_{\min} \le \kappa \le \kappa_{\max}, \\ &0 < (\kappa B_1)_{\min} \le \kappa B_1 \le (\kappa B_1)_{\max}, \\ &(\kappa B_2)_{\min} \le \kappa B_2 \le (\kappa B_2)_{\max} < 0. \end{aligned}$$

Then, we can rewrite (1) as

$$\tau(t) = B(u_d) = \kappa u_d(t) + D(u_d), \tag{2}$$

where $D(u_d)$ denotes a nonlinearity error for the backlash described as

$$D(u_d) = \begin{cases} -\kappa B_1, & \text{if} \quad \dot{u}_d > 0 \quad \text{and} \\ & \tau(t) = \kappa(u_d(t) - B_1), \\ -\kappa B_2, & \text{if} \quad \dot{u}_d < 0 \quad \text{and} \\ & \tau(t) = \kappa(u_d(t) - B_2), \\ \tau(t\_) - \kappa u_d(t), & \text{otherelse}. \end{cases} \tag{3}$$

Remark 1 From the Assumption 1, we derive that $\|D(u_d)\| < D^*$ is bounded and the unknown parameter D^* satisfies $D^* = \max\{(\kappa B_1)_{\max}, -(\kappa B_2)_{\min}\}$.

The schematic diagram of a 2-DOF helicopter is displayed in Fig. 2. From which, it can be observed that the pitch and yaw motions are controlled by the thrust forces F_p and F_y, respectively.

By Lagrange dynamic equations, the nonlinear equations of a 2-DOF helicopter system can be modeled as [32]:

$$\begin{aligned} (J_p + mL_{cm}^2)\ddot{\theta} &= K_{pp}V_p + K_{py}V_y - mgL_{cm}\cos\theta \\ &\quad - D_p\dot{\theta} - mL_{cm}^2\dot{\psi}^2\sin\theta\cos\theta, \end{aligned} \tag{4}$$

$$\begin{aligned} (J_y + mL_{cm}^2\cos^2\theta)\ddot{\psi} &= K_{yp}V_p + K_{yy}V_y - D_y\dot{\psi} \\ &\quad + 2mL_{cm}^2\dot{\psi}\dot{\theta}\sin\theta\cos\theta, \end{aligned} \tag{5}$$

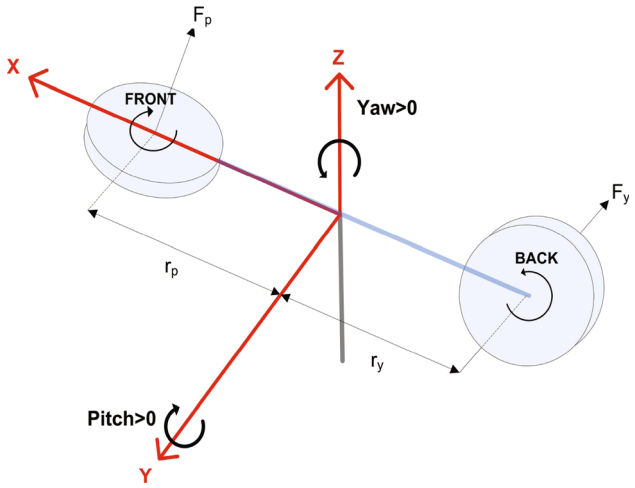

Fig. 2 The schematic diagram of a 2-DOF helicopter

where the specific parameters above-mentioned can be referred in Table 1.

Define the state vectors as $x_1 = [\theta, \psi]^T$ and $x_2 = [\dot{\theta}, \dot{\psi}]^T$, and an input vector as $\tau = [V_p, V_y]^T$. To facilitate the control design, the dynamic Eqs. (4) and (5) can be rewritten as the state-space equations formulated as

$$\begin{aligned} \dot{x}_1 &= x_2, \\ \dot{x}_2 &= F(x_1, x_2) + M(x_1)\tau, \\ y &= x_1, \\ \tau &= B(u_d), \end{aligned} \tag{6}$$

where $\tau = B(u_d)$ denotes the a backlash nonlinearity of the actuators and

Table 1 Parameters of 2-DOF helicopter system

Symbol	Definition
J_p	Moment of inertia about the pitch axis
J_y	Moment of inertia about the yaw axis
D_p	Pitch viscous friction constant
D_y	Yaw viscous friction constant
K_{pp}	Torque thrust gain of F_p acting on pitch axis
K_{py}	Torque thrust gain of F_y acting on pitch axis
K_{yp}	Torque thrust gain of F_p acting on yaw axis
K_{yy}	Torque thrust gain of F_y acting on yaw axis
L_{cm}	Center of mass distance from the body-fixed frame origin
m	Mass

$$F(x_1,x_2)=\begin{bmatrix}\frac{a_2}{a_1}\\ \frac{b_2}{b_1}\end{bmatrix},\quad M(x_1)=\begin{bmatrix}\frac{Kpp}{a_1} & \frac{Kpy}{a_1}\\ \frac{Kyp}{b_1} & \frac{Kyy}{b_1}\end{bmatrix}, \tag{7}$$

with the variables a_1, a_2, b_1 and b_2 designed as

$$a_1=J_p+mL_{cm}^2, \tag{8}$$

$$a_2=-mgL_{cm}\cos\theta-D_p\dot{\theta}-mL_{cm}^2\dot{\psi}^2\sin\theta\cos\theta, \tag{9}$$

$$b_1=J_y+mL_{cm}^2\cos^2\theta, \tag{10}$$

$$b_2=-D_y\dot{\psi}+2mL_{cm}^2\dot{\psi}\dot{\theta}\sin\theta\cos\theta. \tag{11}$$

In practical application, the system nonlinearity and parameters in 2-DOF helicopter systems are difficult to measure accurately, and the functions $F(x_1,x_2)$ and $M(x_1)$ are uncertain, which raises the difficulties in control design. To deal with this, (6) can be rewritten as

$$\begin{aligned}&\dot{x}_1=x_2,\\ &\dot{x}_2=F(x_1,x_2)+\Delta F(x_1,x_2)+(M(x_1)+\Delta M(x_1))\tau,\\ &y=x_1,\\ &\tau=B(u_d).\end{aligned} \tag{12}$$

For the convenience of reading, we replace $F(x_1,x_2)$, $M(x_1)$, $\Delta F(x_1,x_2)$, and $\Delta M(x_1)$ with F, M, ΔF, and ΔM, respectively.

Lemma 1 *The RBFNNs can approximate any continuous unknown function* $f(\zeta)$: $\mathbb{R}^k\rightarrow\mathbb{R}$ [33] *and can be described as*

$$f(\zeta)=W^{*T}S(\zeta)+\epsilon, \tag{13}$$

where $\zeta\subset\mathbb{R}^k$ *represents a RBFNN input vector,* $\hat{W}\in\mathbb{R}^n$ *is an estimated weight vector, and* $n>1$ *is the number of hidden layer nodes.* $S(\zeta)$ *is the basic function expressed as*

$$S(\zeta)=\exp\left[\frac{-(\zeta-C)^T(\zeta-C)}{b^2}\right], \tag{14}$$

where C denotes a RBFNN center vector of the receptive field, and b denotes the width of the Gaussian function.

Lemma 2 *For any positive constant* $k_a\in\mathbb{R}$ *satisfying* $x\in\mathbb{R}$ *and* $\|x\|<\|k_a\|$, *the following inequality holds* [34]

$$\log\frac{k_a^2}{k_a^2-x^2}\le\frac{x^2}{k_a^2-x^2}. \tag{15}$$

3 Control design and stability analysis

Based on backstepping approach, we design the output tracking errors z_1 and z_2, and an auxiliary variable α as follows

$$\begin{aligned}&z_1=x_1-y_d,\\ &z_2=x_2-\alpha,\\ &\alpha=-c_1z_1+\dot{y}_d,\end{aligned} \tag{16}$$

where $c_1=\mathrm{diag}[\mathrm{c11},\mathrm{c12}]$ is a positive definite diagonal matrix.

Combining (12), we provide the time derivative of z_1 and z_2 as

$$\dot{z}_1=x_2-\dot{y}_d=\alpha-\dot{y}_d+z_2=-c_1z_1+z_2, \tag{17}$$

$$\dot{z}_2=\dot{x}_2-\dot{\alpha}=F+\Delta F+(M+\Delta M)\tau-\dot{\alpha}. \tag{18}$$

Considering that the control gain matrix M may be irreversible [35], we define $u_d(t)=M^T\upsilon$, with υ being a designed control input signal, and an appropriate positive parameter λ is selected to make the matrix $(MM^T+\lambda I_{2\times2})$ reversible, with $I_{2\times2}$ being second order identity matrix. Then, with $\tau(t)=\kappa u_d(t)+D(u_d)$ in (2), (18) can be given by

$$\begin{aligned}\dot{z}_2&=F+\Delta F+(M+\Delta M)(\kappa u_d(t)+D(u_d))-\dot{\alpha}\\ &=F+\kappa Mu_d(t)+\Delta F+\kappa\Delta Mu_d(t)\\ &\quad+(M+\Delta M)D(u_d)-\dot{\alpha}\\ &=F+\kappa\left(MM^T+\lambda I_{2\times2}\right)\upsilon-\kappa\lambda I_{2\times2}\upsilon+\Delta F\\ &\quad+\kappa\Delta Mu_d(t)+(M+\Delta M)D(u_d)-\dot{\alpha}.\end{aligned} \tag{19}$$

We consider the Lyapunov function as

$$V_1=\frac{1}{2}\sum_{i=1}^{2}\log\frac{k_{ai}^2}{k_{ai}^2-z_{1i}^2}. \tag{20}$$

Invoking (17), the time derivative of V_1 is described as

$$\dot{V}_1=\sum_{i=1}^{2}\left(\frac{z_{1i}z_{2i}}{k_{ai}^2-z_{1i}^2}-\frac{c_{1i}z_{1i}^2}{k_{ai}^2-z_{1i}^2}\right). \tag{21}$$

To eliminate $\sum_{i=1}^{2}\frac{z_{1i}z_{2i}}{k_{ai}^2-z_{1i}^2}$ in (21), we construct a new Lyapunov function as

$$V_2=\frac{1}{2}\sum_{i=1}^{2}\log\frac{k_{ai}^2}{k_{ai}^2-z_{1i}^2}+\frac{1}{2}z_2^Tz_2. \tag{22}$$

Differentiating (22) yields

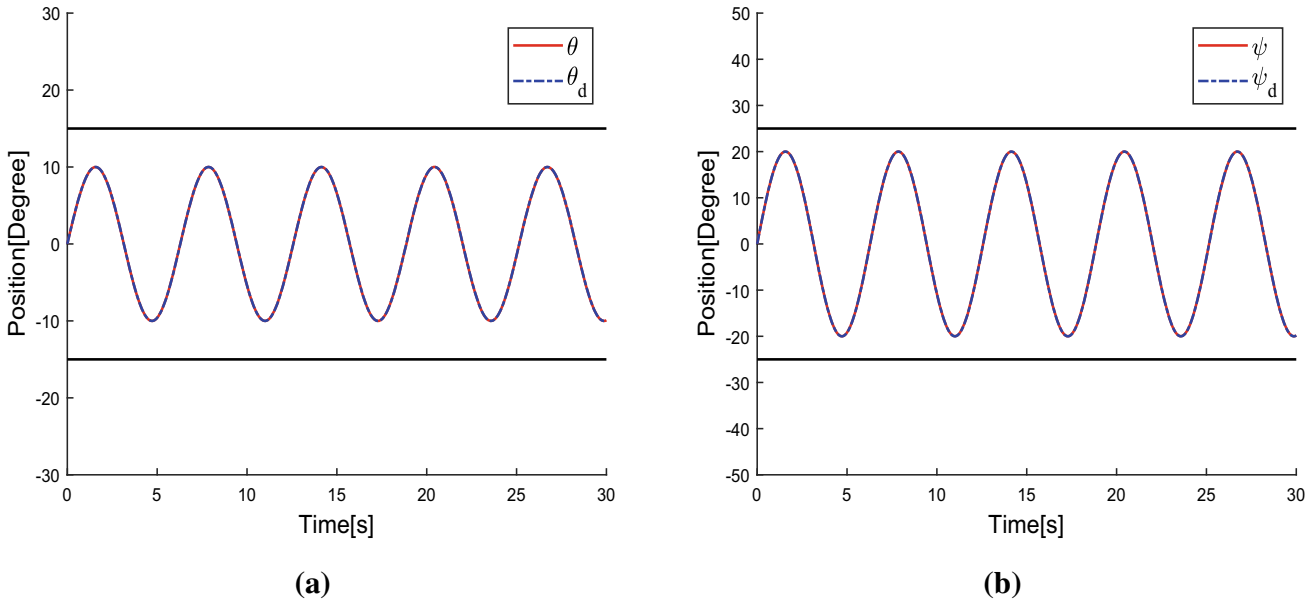

Fig. 3 Simulated tracking performance under the ANNIBOCC: **a** θ, **b** ψ

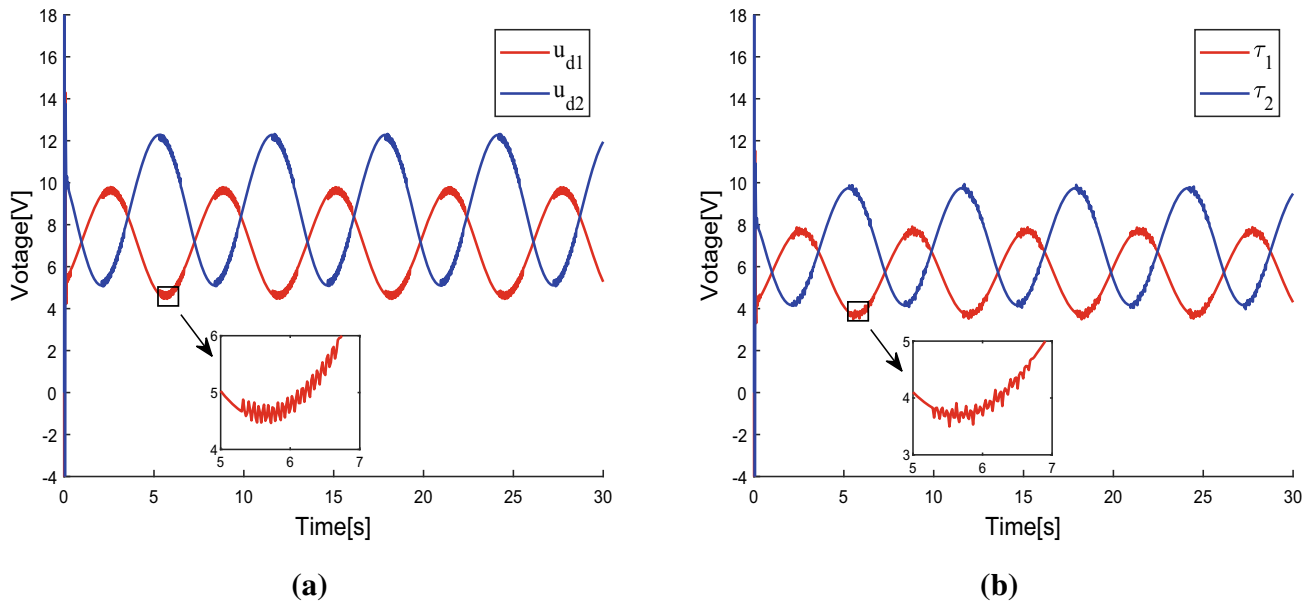

Fig. 4 Simulated input signal under the ANNIBOCC **a** u_d, **b** τ

$$\dot{V}_2 = \sum_{i=1}^{2}\left(\frac{z_{1i}z_{2i}}{k_{ai}^2 - z_{1i}^2} - \frac{c_{1i}z_{1i}^2}{k_{ai}^2 - z_{1i}^2}\right) + z_2^T\left[F + \kappa\left(MM^T + \lambda I_{2\times 2}\right)\upsilon - \kappa\lambda I_{2\times 2}\upsilon + \Delta F + \kappa\Delta M u_d(t) + (M + \Delta M)D(u_d) - \dot{\alpha}\right]. \tag{23}$$

Invoking (23), the following RBFNN is adopted to approximate the unknown function and uncertainties of the system

$$\begin{aligned} f(\zeta) &= W^{*T}S(\zeta) + \epsilon^* \\ &= -\kappa\lambda I_{2\times 2}\upsilon + \Delta F \\ &\quad + \kappa\Delta M u_d(t) + (M + \Delta M)D(u_d) - \dot{\alpha}, \end{aligned} \tag{24}$$

where W^* is an optimal weight vector, ϵ^* is the optimal approximate error, and $S(\zeta)$ is the basis function vector with the input vector $\zeta = [x_1^T, x_2^T, \dot{\alpha}^T, u_d^T]$.

Then, the designed control signal υ can be formulated as

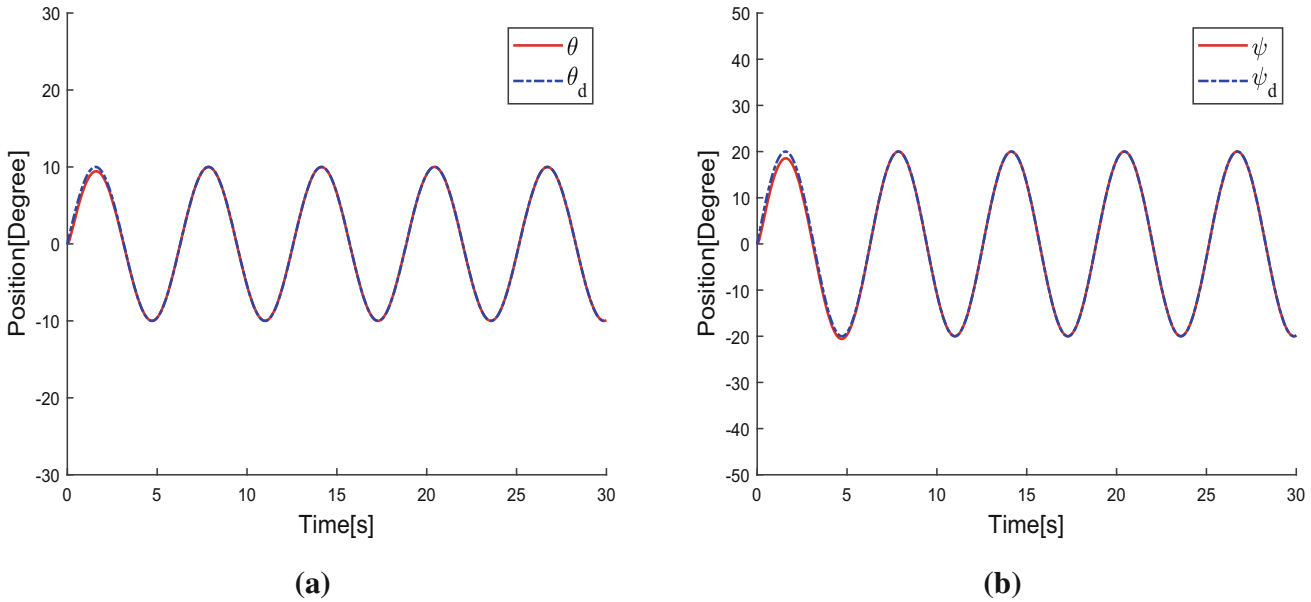

Fig. 5 Simulated tracking performance under the SMC: **a** θ, **b** ψ

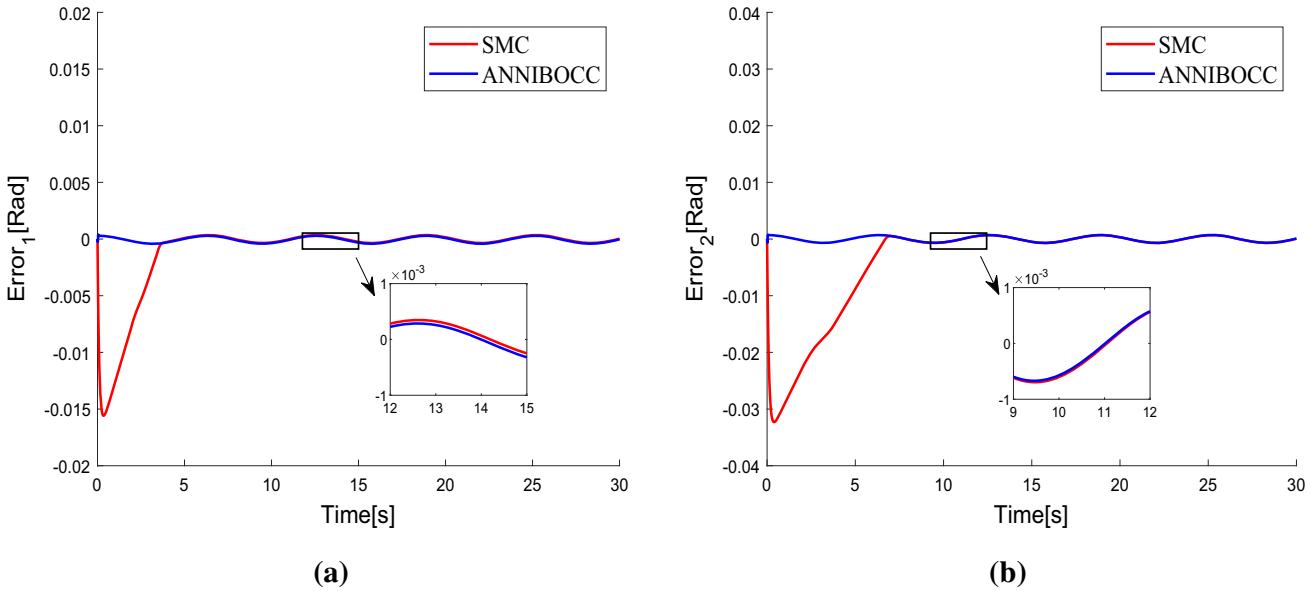

Fig. 6 Simulated tracking errors under the SMC and the ANNIBOCC

$$\upsilon = -\frac{1}{\kappa}(MM^T + \lambda I_{2\times 2})^{-1}\left(c_2 z_2 + F + \begin{bmatrix} \frac{z_{11}}{k_{a1}^2 - z_{11}^2} \\ \frac{z_{12}}{k_{a2}^2 - z_{12}^2} \end{bmatrix} + W^{*T} S(\zeta) + \epsilon^*\right). \tag{25}$$

Considering that the optiaml weight W^* is unknown, the estimated weight $\hat{W}$ is used to approximate it. Hence, the designed control signal υ can be described as follows

$$\upsilon = -\frac{1}{\kappa}(MM^T + \lambda I_{2\times 2})^{-1}\left(c_2 z_2 + F + \begin{bmatrix} \frac{z_{11}}{k_{a1}^2 - z_{11}^2} \\ \frac{z_{12}}{k_{a2}^2 - z_{12}^2} \end{bmatrix} + \hat{W}^T S(\zeta)\right). \tag{26}$$

where c_2 is a positive definite diagonal matrix, and $\hat{W}$ is an estimated weight satisfying $\hat{W} = \tilde{W} + W^*$ with $\tilde{W}$ being a weight error.

Furthermore, we propose an adaptive law as

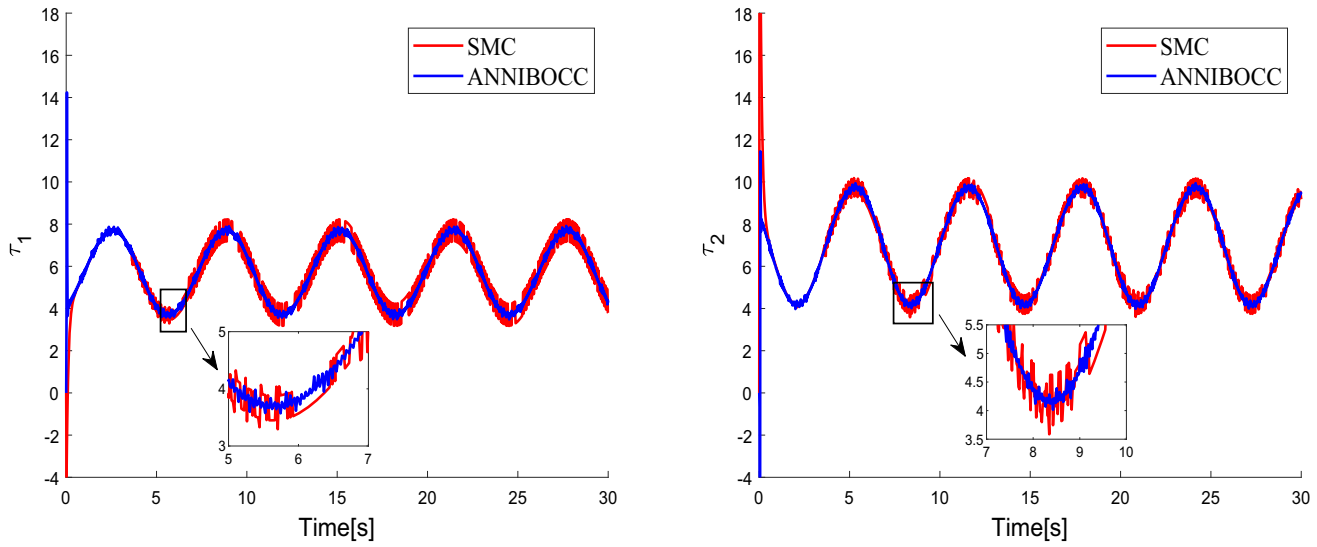

Fig. 7 Simulated input signal τ under the SMC and the ANNIBOCC

$$\dot{\hat{W}} = -\Gamma(z_2^T S(\zeta) + \sigma\hat{W}). \tag{27}$$

where σ is a small postive constant.

Remark 2 Different from the literatures [36, 37], the adaptive neural control method was applied for a class of switched nonlinear systems, to construct a finite-time fault-tolerant controller for handling the tracking problem or construct a novel mode-dependent adaptive laws and sampled-data control laws for stabilizing the controlled system. However, in this paper, we exploit the adaptive neural control method to develop a continous control law for a nonlinear 2-DOF helicopter system for achieving an excellent control performance and guarantee the output contraints satifaction. In addition, when the RBFNN was employed to approximate the unknown dynamic uncertainties and the backlash error in (24), the possiblity of singularity problem caused by the affine item was taken into considertion in (19).

Proof The Lyapunov function for stability analysis is constructed as

$$V = \frac{1}{2}\sum_{i=1}^{2}\log\frac{k_{ai}^2}{k_{ai}^2 - z_{1i}^2} + \frac{1}{2}z_2^T z_2 + \frac{1}{2}tr(\tilde{W}^T\Gamma^{-1}\tilde{W}). \tag{28}$$

Combining (23)–(27), we obtain

$$\begin{aligned}
\dot{V} &= \sum_{i=1}^{2}\frac{z_{1i}\dot{z}_{1i}}{k_{ai}^2 - z_{1i}^2} + z_2^T\dot{z}_2 + tr(\tilde{W}^T\Gamma^{-1}\dot{\tilde{W}}) \\
&= -\sum_{i=1}^{2}\frac{c_{1i}z_{1i}^2}{k_{ai}^2 - z_{1i}^2} + tr(\tilde{W}^T\Gamma^{-1}\dot{\hat{W}}) + \sum_{i=1}^{2}\frac{z_{1i}z_{2i}}{k_{ai}^2 - z_{1i}^2} + \\
&\quad z_2^T[F + \kappa(MM^T + \lambda I_{2\times 2})\upsilon - \kappa\lambda I_{2\times 2}\upsilon + \\
&\quad \Delta F + \kappa\Delta M u_d(t) + (M + \Delta M)D(u_d) - \dot{\alpha}] \\
&\le -\sum_{i=1}^{2}\log c_{1i}\frac{k_{ai}^2}{k_{ai}^2 - z_{1i}^2} - z_2^T(c_2 - \frac{1}{2}I_{2\times 2})z_2 + \frac{1}{2}\|\epsilon*\|^2 \\
&\quad - \frac{\sigma}{2\lambda_{\max}(\Gamma^{-1})}tr(\tilde{W}^T\Gamma^{-1}\tilde{W}) + \frac{\sigma}{2}\|W^*\|^2 \\
&\le -\rho V + \mu
\end{aligned} \tag{29}$$

where

$$\begin{aligned}
\rho &= \min\left(\lambda_{\min}(c_1), \lambda_{\min}(c_2 - \frac{1}{2}I_{2\times 2}), \frac{\sigma}{2\lambda_{\max}(\Gamma^{-1})}\right), \\
\mu &= \frac{1}{2}\|\epsilon^*\|^2 + \frac{\sigma}{2}\|W^*\|^2.
\end{aligned} \tag{30}$$

If the corresponding design matrices c_1, $c_2 - \frac{1}{2}I_{2\times 2}$, and $\frac{\sigma}{2\lambda_{\max}(\Gamma)}$ are chosen to make $\rho > 0$ and the bounded initial states exist, the variables z_1, z_2, and $\tilde{W}$ are semi-globally uniformly ultimately bounded (SGUUB) [38]. We then obtain

$$0 \le V \le \frac{\mu}{\rho} + \left[V(0) - \frac{\mu}{\rho}\right]e^{-\rho t}. \tag{31}$$

Then, we further derive

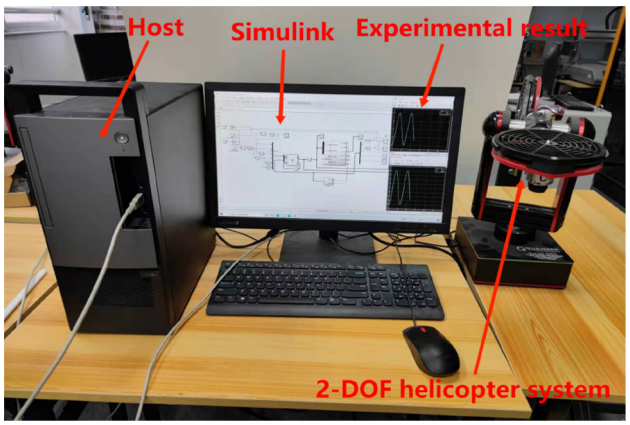

Fig. 8 The Quanser's 2-DOF helicopter platform

$$\begin{aligned} \|z_{1i}\|^2 &\leq k_{ai}^2(1-e^{-2(V(0)+\frac{\mu}{\rho})}),\\ \|z_2\|^2 &\leq 2\left(V(0)+\frac{\mu}{\rho}\right),\\ \|\tilde{W}\|^2 &\leq \frac{2\left(V(0)+\frac{\mu}{\rho}\right)}{\lambda_{min}(\Gamma^{-1})}. \end{aligned} \tag{32}$$

At this moment, we can conclude that the controlled system is SUGGB.

4 Simulation and experiment results

To verify the feasibility and effectiveness of the designed control scheme, we carry out a simulation on the Matlab platform. To further prove the validity and efficacy of the derived control, comparative experiments of two control schemes are conducted on a Quanser's 2-DOF helicopter platform shown in Fig. 8. The two schemes for comparison include adaptive NN with input backlash and output constraint control (ANNIBOCC) and SMC.

4.1 Simulation

In the simulation, the initial states are chosen as $x_1 = [0,0]^T$ and $x_2 = [0,0]^T$. $y_d = [10\pi\sin(t)/180, 20\pi\sin(t)/180]^T$ is a desired tracking trajectory. The relevant parameters for the input backlash are set as $\kappa = 0.8$, $B_1 = 0.2$, and $B_2 = -0.25$. The adaptive law parameters are $\Gamma = 3$ and $\sigma = 0.01$. The control gains are selected as $c_1 = \text{diag}[100, 100]$ and $c_2 = \text{diag}[150, 100]$. The control parameter is given as $\lambda = 0.1$. According the approximated function and the input vector of RBFNN, the nodes are chosen as 150 and the center parameters are chosen as either 1 or -1. The variances are chosen as $b = 2$ and the intial weights $\hat{W}$ are set as zero. The 2-DOF helicopter system parameters are chosen as $J_p = 0.0219$ kg·m^2, $J_y = 0.022$ kg·m^2, $D_p = 0.0071$ N/V, $D_y = 0.022$ N/V, $K_{pp} = 0.0011$ N·m/V, $K_{py} = 0.0022$ N·m/V, $K_{yp} = -0.0027$ N·m/V, $K_{yy} = 0.0022$ N·m/V, $L_{cm} = 0.0071$ m and $m = 1.075$ kg. In Fig. 3, we observe that the output signals of θ and ψ can realize the trajectory tracking with small tracking errors shown in Fig. 6. In other words, the proposed control scheme achieves an excellent control performance in the 2-DOF helicopter system. In addition, the trajectories of θ and ψ are kept within the specified constraint range, which denotes that the output constraints are not violated. It can be depicted from Fig. 4 that the

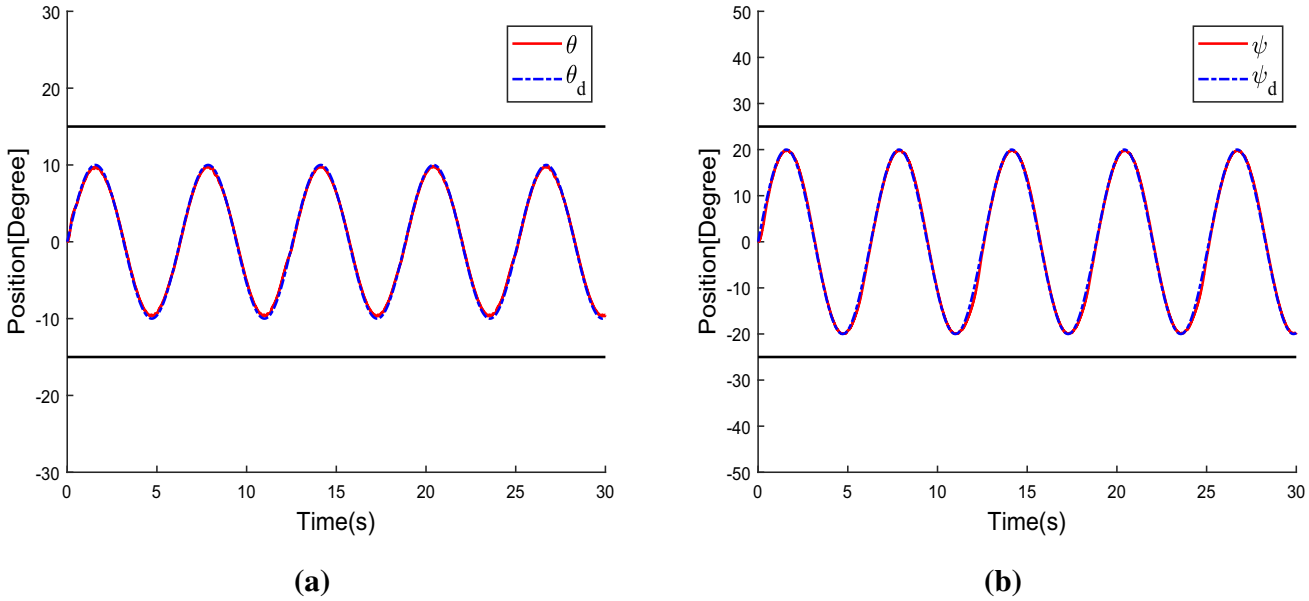

Fig. 9 Tracking performance under the ANNIBOCC: **a** θ, **b** ψ

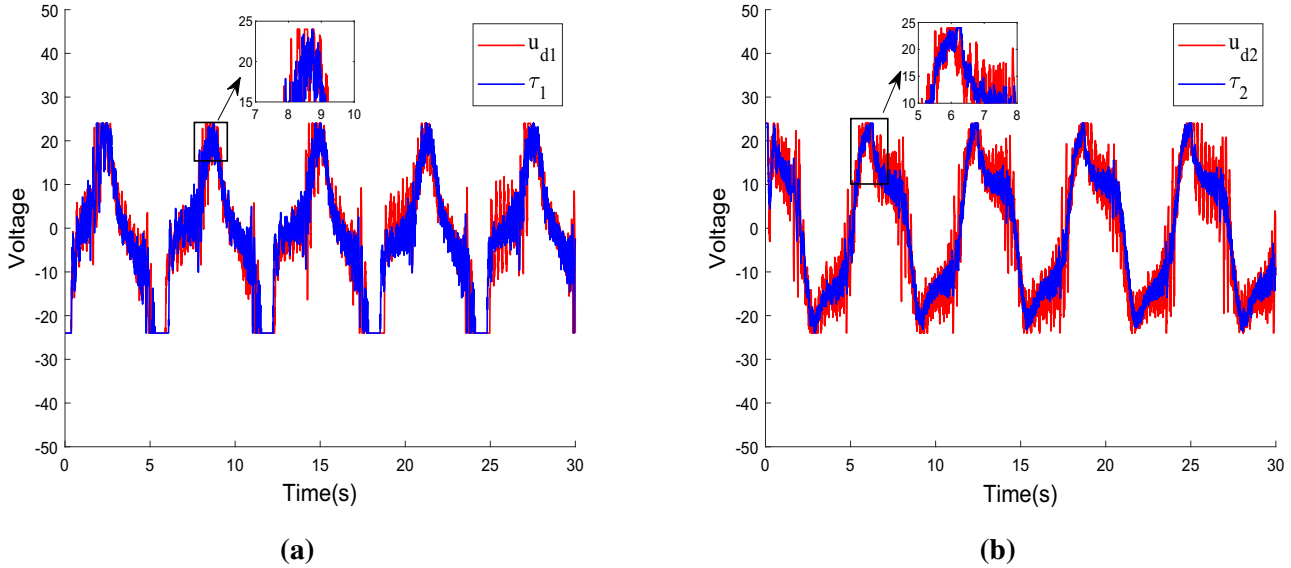

Fig. 10 The contrast picture of u_d and τ under the ANNIBOCC

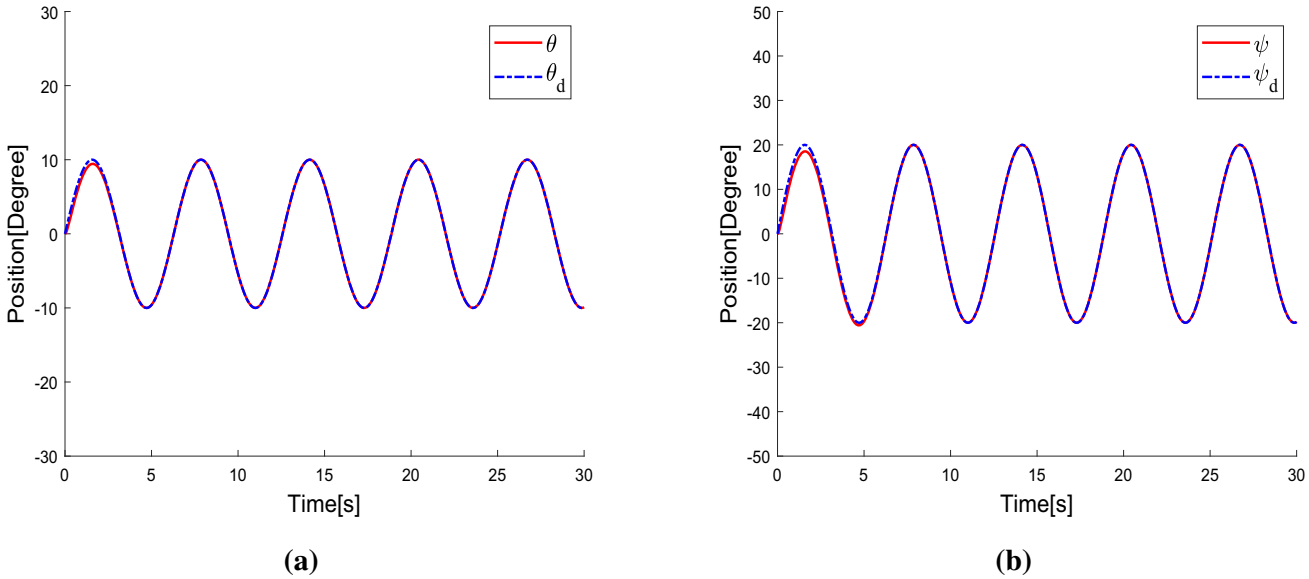

Fig. 11 Tracking performance under the SMC: **a** θ, **b** ψ

input signals become smoother, which illustrates the presented control scheme is capable of eliminating the input backlash nonlinearity. Combining the tracking trajectories under the SMC in Fig. 5 and tracking errors in Fig. 6, we can conclude that the ANNIBOCC scheme achieved a superior control perforamance. As shown in Fig. 7, the appearance of chattering is inevitable under the SMC, which results in more complex input nonlinearity compared with the proposed scheme.

4.2 Experiment

In this part, Figs. 9, 10, 11, 12 and 13 show the experiment results of two nonlinear control schemes, including the ANNIBOCC and SMC. In addition, Fig. 9 depicts the tracking trajectories of θ and ψ under the ANNIBOCC. From which, we can conclude that the proposed scheme ensures no violation of output constraints. In Fig. 10, by comparing the input u_d and τ, we can observe that the processed input τ with backlash nonlinearity is smoother. Figure 11 displays the tracking trajectories under

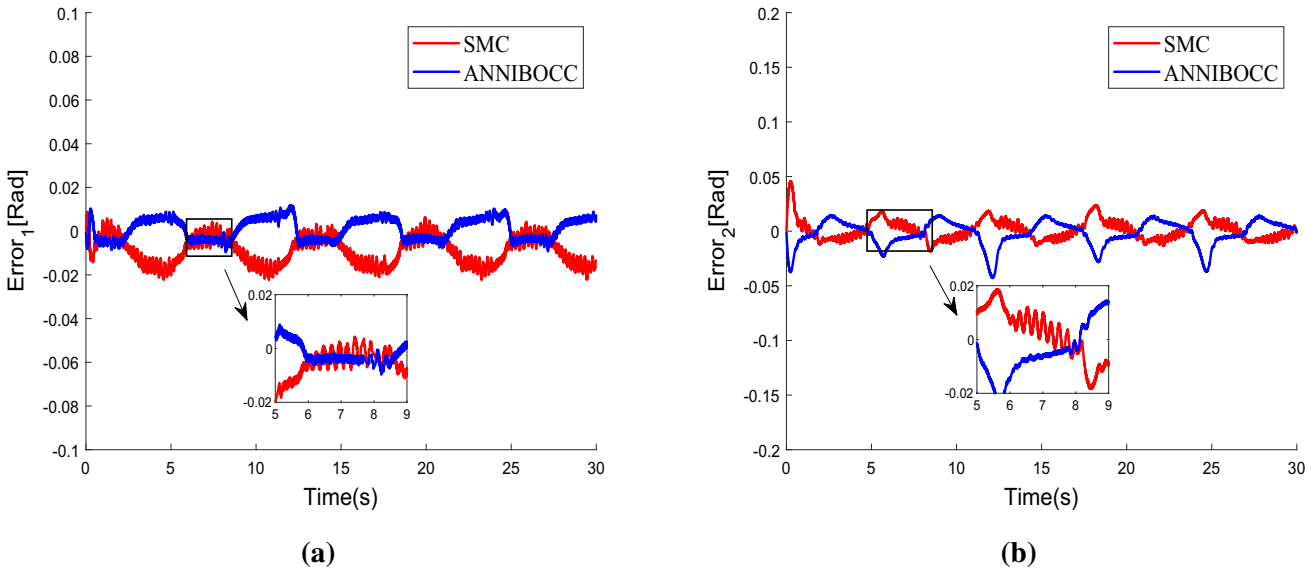

Fig. 12 Tracking errors under the SMC and the ANNIBOCC

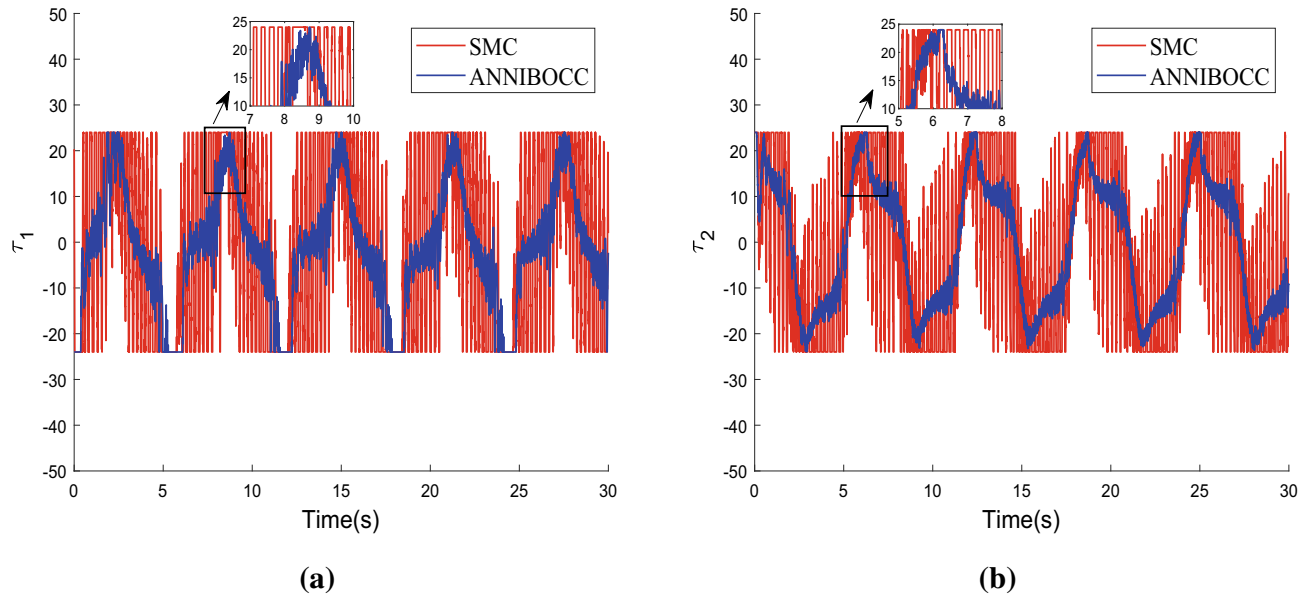

Fig. 13 Input signal τ under the SMC and the ANNIBOCC

the SMC. It can be seen from Figs. 12 and 13 that the tracking errors and input signals demonstrate that the yaw action and pitch action have a drastic chattering, which is caused by the nonlinear mechanism and the characteristics of the SMC algorithm. Under the hybrid effects of chattering and input backlash nonlinearity, rapidly changing inputs are required under the SMC to minimize the tracking errors. This may cause damage to objects with limited input. To sum up, the proposed strategy can effectively eliminate the backlash of input signals and the constrained output ensures that the output signals are retained within a desired range. From the perspective of practical application, the ANNIBOCC with less chattering and smoother input, is more suitable than the SMC.

5 Conclusion

The framework of the adaptive NN control of 2-DOF helicopter systems with input backlash and output constraints was presented in this study. To compensate for the hybrid effects of input backlash nonlinearity and system

uncertainties, the unknown function and nonlinearity error were approximated using the RBFNN. The proposed control scheme realized that the tracking errors converged to a small neighborhood around zero and the backlash was eliminated. Furthermore, the BLF function was adopted to tackle the output constraints, and guarantee the system safety and effectiveness in the operation. Exploiting the rigorous Lyapunov analysis, the designed control realized the controlled system's uniform stability. The simulation and experimental results validated that the designed control revealed a superior control performance. Considering that the output constraints may be asymmetric under certain circumstances and the compensation of the backlash nonlinearity can be futhur improved, the future research will therefore come up with a new approach to address this challenge.

Funding This work was supported by the Scientific Research Projects of Guangzhou Education Bureau under Grant No. 202032793.

Data availability The datasets generated during and/or analysed during the current study are available from the corresponding author on reasonable request.

Declarations

Conflict of interest We declare that we do not have any commercial or associative interest that represents a conflict of interest in connection with the work submitted.

References

1. He W, Wang T, He X, Yang L-J, Kaynak O (2020) Dynamical modeling and boundary vibration control of a rigid-flexible wing system. IEEE/ASME Trans Mechatron 25(6):2711–2721
2. Ulus A, Eski K (2021) Neural network and fuzzy logic-based hybrid attitude controller designs of a fixed-wing UAV. Neural Comput Appl 5:1–23
3. Zhao Z, Zhang J, Liu Z, Mu C, Hong K-S (2022) Adaptive neural network control of an uncertain 2-dof helicopter with unknown backlash-like hysteresis and output constraints. IEEE Trans Neural Netw Learn Syst (**in press**)
4. Raptis IA, Valavanis KP, Vachtsevanos GJ (2012) Linear tracking control for small-scale unmanned helicopters. IEEE Trans Control Syst Technol 20(4):995–1010
5. Nuthi P, Subbarao K (2016) Experimental verification of linear and adaptive control techniques for a two degrees-of-freedom helicopter. J Dyn Syst Meas Control 137(6):064501
6. Subramanian RG, Elumalai VK (2016) Robust mrac augmented baseline lqr for tracking control of 2 dof helicopter. Robot Auton Syst 86:70–77
7. Chun TY, Park JB, Choi YH (2018) Reinforcement q-learning based on multirate generalized policy iteration and its application to a 2-dof helicopter. Int J Control Autom Syst 16:377–386
8. Butt SS, Sun H, Aschemann H (2015) Control design by extended linearisation techniques for a two degrees of freedom helicopter. Ifac Papersonline 48(11):22–27
9. Yuan Y, Cheng L, Wang Z, Sun C (2019) Position tracking and attitude control for quadrotors via active disturbance rejection control method. Science China (Inf Sci) 62(1):10
10. He W, Mu X, Zhang L, Zou Y (2021) Modeling and trajectory tracking control for flapping-wing micro aerial vehicles. IEEE/CAA J Autom Sin 8(1):148–156
11. Ouyang Y, Dong L, Xue L, Sun C (2019) Adaptive control based on neural networks for an uncertain 2-dof helicopter system with input deadzone and output constraints. IEEE/CAA J Autom Sin 6(3):807–815
12. Zeghlache S, Kara K, Saigaa D (2014) Type-2 fuzzy logic control of a 2-dof helicopter (TRMS system). Open Eng 4(3):303
13. Hernandez-Gonzalez M, Alanis AY, Hernandez-Vargas EA (2012) Decentralized discrete-time neural control for a quanser 2-dof helicopter. Appl Soft Comput 12(8):2462–2469
14. Zhang J, Cheng X, Zhu J (2016) Control of a laboratory 3-dof helicopter: explicit model predictive approach. Int J Control Autom Syst 14(2):389–399
15. Meza-Sánchez M, Aguilar LT, Orlov Y (2015) Output sliding mode-based stabilization of underactuated 3-dof helicopter prototype and its experimental verification. J Frankl Inst 352(4):1580–1594
16. Zhou J, Zhang C, Wen C (2007) Robust adaptive output control of uncertain nonlinear plants with unknown backlash nonlinearity. IEEE Trans Autom Control 52(3):503–509
17. Yang C, Huang D, He W, Cheng L (2021) Neural control of robot manipulators with trajectory tracking constraints and input saturation. IEEE Trans Neural Netw Learn Syst 32(9):4231–4242
18. Zhao Z, Liu Z, He W, Hong K-S, Li H-X (2021) Boundary adaptive fault-tolerant control for a flexible timoshenko arm with backlash-like hysteresis. Automatica 130:109690
19. Yan H, Li Y (2015) Adaptive nn prescribed performance control for nonlinear systems with output dead zone. Neural Comput Appl 28(1):1–9
20. Mousavi SH, Ranjbar-Sahraei B, Noroozi N (2012) Output feedback controller for hysteretic time-delayed mimo nonlinear systems an h-infinity-based indirect adaptive interval type-2 fuzzy approach. Nonlinear Dyn 68(2):76–78
21. Yu J, Shi P, Liu J, Lin C (2020) Neuroadaptive finite-time control for nonlinear mimo systems with input constraint. IEEE Trans Cybern 1–8
22. Hegde N, George V, Nayak C, Vaz A (2021) Application of robust h-infinity controller in transition flight modeling of autonomous vtol convertible quad tiltrotor uav. Int J Intell Unmanned Syst 9(3):204–235
23. Huang D, Yang C, Pan Y, Cheng L (2021) Composite learning enhanced neural control for robot manipulator with output error constraints. IEEE Trans Ind Inform 17(1):209–218
24. Zhao Z, Ahn CK, Li H-X (2020) Dead zone compensation and adaptive vibration control of uncertain spatial flexible riser systems. IEEE/ASME Trans Mechatron 25(3):1398–1408
25. Zhao Z, Ren Y, Mu C, Zou T, Hong K-S (2021) Adaptive neural-network-based fault-tolerant control for a flexible string with composite disturbance observer and input constraints. IEEE Trans Cybern 1–11
26. Zhao Z, Liu Y, Zou T, Hong K-S, Li H-X (2022) Robust adaptive fault-tolerant control for a riser-vessel system with input hysteresis and time-varying output constraints. IEEE Trans Cybern (**in press**)
27. He W, Huang H, Ge SS (2017) Adaptive neural network control of a robotic manipulator with time-varying output constraints. IEEE Trans Cybern 47(10):3136–3147
28. Li DP, Liu YJ, Tong S, Chen CLP, Li DJ (2019) Neural networks-based adaptive control for nonlinear state constrained systems with input delay. IEEE Trans Cybern 49(4):1249–1258

29. Liu YJ, Tong S, Chen CLP, Li DJ (2017) Adaptive nn control using integral barrier Lyapunov functionals for uncertain nonlinear block-triangular constraint systems. IEEE Trans Cybern 47(11):3747–3757
30. Liu Y-J, Lu S, Tong S (2017) Neural network controller design for an uncertain robot with time-varying output constraint. IEEE Trans Syst Man Cybern Syst 47(8):2060–2068
31. He X, Zhao Z, Su J, Yang Q, Zhu D (2021) Adaptive inverse control of a vibrating coupled vessel-riser system with input backlash. IEEE Trans Syst Man Cybern Syst 51(8):4706–4715
32. Xin Y, Qin ZC, Sun JQ (2018) Input-output tracking control of a 2-dof laboratory helicopter with improved algebraic differential estimation. Mech Syst Signal Process 116:843–857
33. Ge SS, Wang C (2004) Adaptive neural control of uncertain mimo nonlinear systems. IEEE Trans Neural Netw 15(3):674–692
34. Zhao Z, He W, Ge SS (2014) Adaptive neural network control of a fully actuated marine surface vessel with multiple output constraints. IEEE Trans Control Syst Technol 22(4):1536–1543
35. Chen M, Shi P, Lim C-C (2016) Adaptive neural fault-tolerant control of a 3-dof model helicopter system. IEEE Trans Syst Man Cybern Syst 46(2):260–270
36. Cui D, Wu Y, Xiang Z (2021) Finite-time adaptive fault-tolerant tracking control for nonlinear switched systems with dynamic uncertainties. Int J Robust Nonlinear Control 31:2976–2992
37. Li S, Ahn CK, Guo J, Xiang Z (2021) Neural network-based sampled-data control for switched uncertain nonlinear systems. IEEE Trans Syst Man Cybern Syst 51(9):5437–5445
38. Chen M, Ge SS, Ren B (2011) Adaptive tracking control of uncertain mimo nonlinear systems with input constraints. Automatica 47(3):452–465